0 0 0 0 4 2 0 2 8 2 6

Submitted to Physics of Fluids

RECEIVED
LAWRENCE
BERKELEY LABORATORY

JUL 21 1975

LIBRARY AND
DOCUMENTS SECTION

LBL-3257
Preprint c.1

STUDY OF PLASMA DENSITY DISTRIBUTION PRODUCED BY IRRADIATING A 50μ DEUTERIUM PELLET ON ONE SIDE WITH A RUBY LASER

T. R. Jarboe, W. B. Kunkel, and A. F. Lietzke

April 1975

Prepared for the U. S. Energy Research and
Development Administration under Contract W-7405-ENG-48

For Reference

Not to be taken from this room

LAWRENCE BERKELEY LABORATORY
UNIVERSITY OF CALIFORNIA
BERKELEY

LBL-3257
c.1

DISCLAIMER

This document was prepared as an account of work sponsored by the United States Government. While this document is believed to contain correct information, neither the United States Government nor any agency thereof, nor the Regents of the University of California, nor any of their employees, makes any warranty, express or implied, or assumes any legal responsibility for the accuracy, completeness, or usefulness of any information, apparatus, product, or process disclosed, or represents that its use would not infringe privately owned rights. Reference herein to any specific commercial product, process, or service by its trade name, trademark, manufacturer, or otherwise, does not necessarily constitute or imply its endorsement, recommendation, or favoring by the United States Government or any agency thereof, or the Regents of the University of California. The views and opinions of authors expressed herein do not necessarily state or reflect those of the United States Government or any agency thereof or the Regents of the University of California.

0 0 0 0 4 2 0 2 8 2 7

STUDY OF PLASMA DENSITY DISTRIBUTION PRODUCED BY IRRADIATING A 50 μ DEUTERIUM PELLET ON ONE SIDE WITH A RUBY LASER*

T.R. Jarboe,† W.B. Kunkel, and A. F. Lietzke

Lawrence Berkeley Laboratory
University of California
Berkeley, California 94720

April 1975

ABSTRACT

Freely falling 50-μm diameter deuterium pellets are irradiated on one side with a ruby laser pulse of 1 ns rise time. It is found that the freely expanding plasma has an asymptotic density distribution which is shell like. The observed laser-pellet interaction time, expansion velocity, and asymptotic density distribution are found to be in good agreement with a simple model for the ablation and acceleration of the pellets. The total number of ions produced is about 5×10^{15}. This is consistent with complete ionization of the 50-μm pellets. The plasma is given an energy on the order of 100 eV per particle when the laser intensity is 10^{12} watts/cm^2.

0 0 0 0 4 2 0 2 8 2 8

INTRODUCTION

Since the invention of the giant pulse laser, scientists have been studying the interaction of intense laser light with matter. Laser-produced plasma can be made by focusing the light in a dense gas[1] or by focusing it onto solid matter. Laser-produced plasmas have been made with thin and thick foils[2,3] as well as with small pellet targets. In "pellet plasmas" the focal spot size of the laser is larger than the target size but for laser produced "foil plasmas" the focal spot is smaller than the target.

The advantage of laser-produced plasmas over others is that they can be very pure. The advantages of pellets over foils and gas targets are that the plasma produced is isolated and can be nearly fully ionized.

In this experiment, 50-μm diameter deuterium pellets are used as the targets for laser irradiation with a focal spot diameter in excess of 100 μm. Some of the advantages of hydrogen or its isotopes as the pellet material are the following: the plasma requires less energy to fully ionize, its recombination and ionization rates are known, and since it has only one stage of ionization, one can count ions by simply measuring charge.

Deuterium pellets of 100-400 μm size have been produced and irradiated.[4-6] However, in order to get a fully ionized plasma of greater than 100-eV ions, using a 10-J laser, it is necessary to use smaller pellets.

Uses for laser-produced pellet plasmas other than the study of the interaction of the plasma with the magnetic field include confinement studies:[6,7] line-tying experiments, instability study, and shock studies. Laser-produced plasmas trapped in a magnetic field can also be used as

targets for neutral beam injection.[8] Another more ambitious use of laser plasma is the creation of miniature thermonuclear explosions by compressing and heating pellets (~ 0.5 mm in diameter) with high-power lasers.[9]

None of the experiments on the expanding plasma reported to date have used truly isolated pure solid hydrogen pellets freely falling in a vacuum and at the same time small enough to become fully ionized. Our techniques of pellet production and irradiation are described elsewhere.[10,11]

Haught, Polk, and Fader have extended a model first proposed by Dawson[12] for the heating and expansion of laser pellet plasmas[13-15] and have compared it to their experiments using LiH pellets.[13,15] In the free-expansion case, using time-of-flight measurements, they found good agreement between experiment and theory for the energy of the plasma as a function of the pellet size and laser pulse width and amplitude. However, the measured asymptotic radial density distribution is not in agreement with the theory. The latter predicts a Gaussian asymptotic density profile while a more shell-like profile was observed.[15]

Although Haught and Polk's model has its weaknesses, it is a good model for very small pellets. From Lubin's[16] data the theory appears to work well for pellets under 25 μm in diameter. Mattioli and Veron have shown that the model does not seem to fit the experimental heating of 50 μm and larger diameter LiH pellets.[17] They have shown experimentally that a square pulse of 20 ns length at 1.5×10^{12} W/cm^2 is required to "burn through" a 50-μm diameter LiH pellet and that a 40 ns pulse is

not long enough for a 120-μm diameter pellet at 1.5×10^{12} W/cm^2. They also show that the expansion is spherically symmetric, if, and only if, the pulse is long enough to burn through the pellet. They tried using an ablation model developed by Caruso and Gratton[18] but did not find good quantitative agreement with the "burn" time. They concluded that more work needed to be done on the theory of heating. We shall use the word "burn" as synonymous with "ablate" in this paper.

A description of the interaction of a ruby laser at $\phi = 10^{12}$ W/cm^2 with a 50-μm deuterium foil is given by Mulser, Sigel, and Witkowski.[19] Qualitatively this description also applies to a pellet hit from one side. The model is a hydrodynamic model with inverse bremsstrahlung as the main heating mechanism accompanied by a compression wave propagating forward and preheating the overdense material. Mulser, et al., have also done some numerical simulations of the interaction of a laser with a 100-μm deuterium pellet, again based on a hydrodynamic model with inverse bremsstrahlung as the heating mechanism. They found for a power flux equal to 5×10^{12} W/cm^2 essentially all the absorption takes place in a region small compared to the dimensions of the pellet and having a density below the critical value n_c. For power less than 5×10^{12} W/cm^2 a substantial fraction of the energy incident on the pellet is absorbed. This computer simulation also includes thermal conductivity, and it was found that for $\phi \lesssim 10^{13}$ W/cm^2 thermal conductivity is of little importance in the heating process.

SIMPLE MODEL OF PLASMA FORMATION AND FREE EXPANSION

In light of the above comments on the role of thermal conduction pertaining to heating of the pellet by a laser, it seems that a model using zero thermal conductivity may better describe the laser pellet interaction. To construct such a model, we will divide it into the following time sequence: (1) early, (2) intermediate, and (3) late. The early time starts with irradiation and ends when the shock reaches the back of the pellet. It is important that the rise-time of the pulse be shorter than this time if our model is to be applicable. The "late" time starts when the pellet becomes translucent to laser light, so that volume absorption sets in, and ends when it becomes completely transpartent. In the following discussion of the detailed physics of the over-dense plasma ($n > n_c$), a one-dimensional model is used. This is justifiable because radial expansion is greatly suppressed by the presence of the laser beam when the pellet is initially much smaller than the focal spot. As the dense plasma (henceforth called the pellet) tries to expand laterally across the laser beam, the density on the edge drops and the interface of laser absorption extends back. Thus, pressure due to ablation is applied to the sides as well and impedes radial expansion of the compressed pellet (see Fig. 1).

1. Early Time

A simple semi-quantitative description of the early interaction of a 50-μm deuterium pellet with a ruby laser at intensities near 10^{12} W/cm^2 can be given by using the assumptions listed below. (Most of these are supported by the results of Mulser, et al.[19] described above.)

(a) All of the absorption takes place in a distance short compared to the pellet dimensions. However, in contrast to Mulser, et al., and to Caruso and Gratton, we assume the absorption to be concentrated in the narrow region where n is near and slightly above n_c.

(b) All of the energy incident on the pellet is absorbed, and thermal conduction is ignorable.

(c) The energy going into the shocked material is small compared to the total amount absorbed in the pellet frame of reference, i.e., most energy is in the ablated material.

(d) Ionization energy and radiated energy are negligible.

(e) All phases of deuterium obey the ideal gas law.

(f) The only forces on the plasma are hydrodynamic in nature.

(g) The deflagration of the pellet due to the laser energy is a Chapman-Jouguet deflagration.[20]

In a Chapman-Jouguet deflagration, the "burn" front observed from the ablated material moves at the sound speed of the expanding material.[20] Thus in the pellet frame the energy flux leaving the pellet is

$$\left(\frac{1}{2} m_i C_c^2 + \frac{5}{2} kT_c\right) n_c C_c = \Phi_L, \tag{1}$$

where m_i = mass of ion, $T_c = T_i + T_e$ at n_c, and C_c is the sound speed at the point where the density is equal to n_c. The laser energy flux Φ_L is assumed constant. Since $C_c^2 = \gamma kT_c/m_i$, with $\gamma = 5/3$ we obtain

$$C_c = \left(\frac{\Phi_L}{2n_c m_i}\right)^{1/3} . \tag{2}$$

This relation can be recognized as similar in form to the result obtained by Bobin, et al.[21] It is much simpler than the latter because we have neglected both the relatively small radiation loss and the internal energy in the compressed pellet, and we have expressed the energy in the (moving) pellet frame. It has the same dependence on Φ_L because both models involve a deflagration process with strong absorption of the incident laser flux in a thin layer of plasma that is already "ablated" and expanding so that its density is dropping just to the critical value, n_c. For these conditions the same result has also been inferred by Puell.[22] If this last simplifying assumption is dropped and the heating, described by classical inverse bremsstrahlung, dominates throughout the underdense streaming plasma, $C_c \propto \Phi_L^{2/9}$ is obtained,[18,19,22] which differs only slightly from our $\Phi_L^{1/3}$.

Finally, because practically the entire energy ends up as kinetic energy of streaming ions, the asymptotic (exhaust) velocity of the evaporated plasma in the pellet frame, V_{ex}, becomes

$$V_{ex} = 2C_c \approx \left(\frac{4\Phi_L}{n_c m_i}\right)^{1/3} . \tag{3}$$

The time to "burn" through the pellet is t_b, where

$$t_b = (L_0/C_c)(n_0/n_c) \tag{4}$$

in which n_0 and L_0 denote the initial density and diameter of the pellet. The shock propagation for a time L_0/V_s, i.e., at the end of the "early time", and the density of the pellet at this time is shown in Ref. 19 (their Fig. 3). At this point, about 1/8 of the pellet is ablated. Note that the original shape of the pellet is relatively unimportant since

the shock-compressed material is in a fluid state and presumably acquires a smooth surface quickly (see Fig. 1). Moreover, the material is flattened by the strong compression so that the one-dimensional model may represent a fair approximation.

2. Intermediate Time

Since there is a vacuum on the left end of the pellet, a complete rarefaction forms with the front edge traveling at $3C_c$ forward.[20] This simple rarefaction wave propagates back through the compressed pellet at the sound speed C_s and finally reaches the deflagration region. Up to this time the density and velocity of the plasma as a function of distance and time are given by Courant and Friedrichs.[20] At this point, about 18% of the pellet is gone and the problem becomes more difficult. However, the evolution can be modeled further by using the results of Courant and Friedrichs as the initial conditions, and the boundary condition that the pressure is constant and the pellet is ablating at the rate necessary to maintain this pressure. Thermal conductivity is ignored and the adiabatic law is used. The results are shown in Fig. 2.

3. Late in Time

After $t/t_b = 0.9$ the thickness of the pellet (full width at half maximum of the density) is about 1 wavelength. Thus the pellet becomes translucent, leading to volume absorption much as described by Haught and Polk.[13] The acceleration stops, resulting in a three-dimensional rapid expansion of the pellet and it soon becomes transparent.

ASYMPTOTIC DENSITY DISTRIBUTION

The quantity which is of the most practical significance and one of the most measurable is the asymptotic[23] density distribution of the

plasma produced by such an interaction. The problem of finding the density distribution in space becomes tractable if the deformations of the pellet described above are ignored and the pellet is assumed hard, in the sense that the velocity is uniform throughout the pellet. If this is the case then the velocity of the pellet is described by the well-known rocket formula

$$V_p = V_{ex} f \ln\left(1 - \frac{t}{t_b}\right), \quad 0 < t \leq t_b \tag{5}$$

where

$$f = \frac{\int_0^\pi \Gamma(\theta_p) V(\theta_p) \cos\theta_p \sin\theta_p \, d\theta_p}{V_{ex} \int_0^\pi \Gamma(\theta_p) \sin\theta_p \, d\theta_p} \tag{6}$$

is the fraction of ablation flux transferring momentum to the pellet along the beam direction. In this expression $\Gamma(\theta_p)$ is the number of ions per steradian per second going into the angle θ_p with velocity $V(\theta_p)$ in the pellet frame. In order to compare V_p to the velocity of the deflagration front in the laboratory frame of the previous model, $f \cdot V_{ex}$ must be set equal to 8/5 C_c. The plot of the velocity of the deflagration front of both models is shown in Fig. 3. For $0.2 < t/t_b < 0.9$ both models give essentially the same result. Thus the hard-pellet model gives a good approximation to the velocity of the deflagration front in the laboratory frame. The greatest differences occur early and late in time.

To proceed with finding the density distribution under this hard-pellet assumption, assume axial symmetry about the laser beam and let θ_L = angle in the laboratory frame with respect to the laser beam. Also assume that $V(\theta_p)$ and $\Gamma(\theta_p)$ are time independent so that f is constant.

From geometry,

$$V(\theta_p)\ \sin\theta_p = V_r\ \sin\theta_L$$

$$V_r\ \cos\theta_L = V(\theta_p)\ \cos\theta_p + V_p$$

$r/t_0 = V_r$ = radial velocity in the laboratory frame.

Now define $N(\theta_p) \equiv \Gamma(\theta_p)t_b$. It can be shown that the asymptotic density distribution is $n(r,\theta_L)$,[10] where

$$n(r,\theta_L) = \frac{N(\theta_p)\ e^{V_p/fV_{ex}}}{V(\theta_p)f\left(\frac{dV(\theta_p)}{d\theta_p}\sin\theta_p + V(\theta_p)\ \cos\theta_p\right)}\ \frac{1}{t_0^{\,3}V_{ex}} \qquad (7)$$

This relationship is used to compare observed density distributions, or rather, plasma fluxes, with simple ablation models.

EXPERIMENTAL RESULTS AND COMPARISONS TO SIMPLE MODEL

The asymptotic density distribution is measured by six coaxial charge collectors and the burn time is measured by two photo diodes. The charge collectors are located 8 cm from the zap zone approximately on the axes of a three-dimensional coordinate system with the laser light coming down one axis. Forward refers to the direction the laser light is propagating and backward is the opposite direction.

The observed probe currents decrease faster than $1/t^4$. Therefore, the density distribution is shell-like and it seems reasonable to fit the data to the above described model. The particle current arriving at a charge collecting probe of solid angle $d\Omega_L$ can be found to be[10]

$$I = \frac{N(\theta_p)}{V(\theta_p)}\ \frac{R^3}{t^4 V_{ex}}\ \frac{1}{f}\ e^{V_p/fV_{ex}}\ \frac{d\Omega_L}{\frac{dV(\theta_p)}{d\theta_p}\sin\theta_p + V(\theta_p)\ \cos\theta_0}. \qquad (8)$$

Figure 4 shows the fit achieved using the hard-pellet model. The fit is a least-squares fit of the probe currents to this equation, with $\Gamma(\theta_p) = A \cos^{\alpha}\theta_p$ and $V(\theta_p) = V_{ex}(1 - B \sin\theta_p)$, where A, B, and α are the fitting parameters and V_{ex} is found by measuring the time of the current peak of the back probe: $V_{ex} \equiv R/t_p$, where R = distance of the probe from the zap zone. A is a normalization constant and α and B parametrize the nature of the deflagration.

In the data analyzed (six typical shots) the value of $\alpha = 2.0 \pm 0.3$ and $B = 0.33 \pm 0.06$. The $\pm$ includes the full range of values found. The asymptotic density distribution from such $N(\theta_p)$ and $V(\theta_p)$ is shown in Fig. 5.

If one assumes that the plasma comes off the pellet normal to the critical surface, where $n = n_c$, and travels in straight lines with respect to the pellet, then by using the experimentally determined $N(\theta_p)$ and $V(\theta_p)$ the shape of the deflagration front can be calculated and the results are incorporated in Fig. 1. The shape is very similar to what would be expected from the discussion of the detailed model.

The sudden change in the rate of fall of the back current signals may be a consequence of the arrival of the rarefaction wave at the deflagration front. The poor fit to the forward probe signal is understood from the description of the late part of the burn. Once the pellet becomes translucent it is so thin that it quickly becomes transparent. Thus, much of the forward going plasma travels at the velocity which the pellet had when translucency occurred and arrives at the probe at the same time, producing the narrow spike. By comparing this pellet velocity to the

exhaust velocity, the time during the burn at which translucency occurs can be measured. The relative time of the forward peak with respect to the back varies slightly from shot to shot and the times of arrival are nearly equal, thus translucency occurs when $V_p \approx V_{ex}$. Now, if $N(\theta_p) \propto \cos^2\theta_p$ and $V(\theta_p) = [1 - (1/3)\sin\theta_p]\, V_{ex}$, we find $f = 0.6$ so that Eq. (5) yields $t \approx 0.8\ t_b$.

At this point, if it were not for lateral expansion, the length of the compressed pellet would be 2.5 μm or about 3.4 free-space wavelengths. This is too thick for translucency. However, if we assume in Fig. 1 that the original pellet corresponds to the nearly vertical portion of the pellet profile, then the average pellet radius has increased about 50%. Thus the area is about doubled and the length of the pellet is halved. This would mean that the pellet is 1.7 wavelengths long at translucence, which is a more reasonable value. It appears to be necessary that the pellet expand before radial confinement becomes effective.

The two photo diodes are calibrated with the help of an optical calorimeter. The difference of the input and output photo diodes is used to measure the burn time, and the amplitude of the input is used to measure the laser power. Figure 6 shows the graph of Eq. (3) for V_{ex} as a function of Φ_L along with measured values of V_{ex} and Φ_L. There seems to be reasonably good agreement here, corroborating the results of Bobin, et al.[21] Figure 7 shows the laser pulse output and the difference signal. The measured absorption time is about 16 ns. Taking into account the radial expansion described above and substituting into Eq. (4), we find

$$t_b = 8.2\ \Phi_L^{-1/3} \qquad (\Phi_L \text{ is in } 10^{12}\ \mathrm{W/cm^2})\ .$$

Now, since the absorbed power is 12 MW, $\Phi_L = 0.2 \times 10^{12}$ and so the expected t_b = 14 ns. Thus, the model and experiment are consistent.

Incidentally, if LiH is the pellet material and Nd glass is used for the laser, then $t_b = 25\ \Phi_L^{-1/3}$ ns. So for 50-μm pellets at $\Phi_L = 1.5 \times 10^{12}$, t_b = 21 ns. This is in good agreement with the experimental results of Mattioli and Veron.[17]

SUMMARY AND CONCLUSIONS

We have made and irradiated on one side, freely falling 50-μm deuterium pellets with a fast rising ruby laser pulse. It was found that the freely expanding plasma had an asymptotic density distribution which was shell-like. The burn time, expansion velocity, and asymptotic density distribution were found to be in good agreement with a simple model of the ablation and acceleration of the pellet.

ACKNOWLEDGMENTS

The authors wish to thank W.R. Baker, K.W. Ehlers, J.E. Galvin, E.B. Hewitt, V.J. Honey, M.L. Fitzgerald, and G.H. Rankin for their advice and assistance.

FOOTNOTES AND REFERENCES

*Work performed under the auspices of the U. S. Energy Research and Development Administration.

†Present address, Los Alamos Scientific Laboratory, Los Alamos, N.M.

1. H.J. Schwarz and H. Hora, Laser Interaction and Related Plasma Phenomena (Plenum Press, New York-London, 1972).
2. P.T. Rumsby and J.W.M. Paul, Plasma Phys. 16, 247 (1974).
3. R. Sigel, Z. Naturforsch. 25a, 488 (1970).
4. U. Ascoli-Bartoli, B. Brunelli, A. Caruso, A. De Angelis, G. Gati, R. Gratton, F. Parlange, and H. Salzmann, Production of a Dense Deuterium Plasma in a Strong Magnetic Field by a Giant Laser Pulse (Hot-Ice Experiment), in Plasma Physics and Controlled Nuclear Fusion Research (International Atomic Energy Agency, Vienna, 1969), Vol. 1, p. 917.
5. G. Francis, D.W. Atkinson, P. Avivi, J.E. Bradley, C.D. King, W. Millar, P.A.H. Saunders, and A.F. Taylor, Phys. Letters A25, 486 (1967).
6. A. Kitsumezaki, M. Tanimoto, and T. Sekiguchi, Phys. Fluids 17, 1895 (1974).
7. A.F. Haught, D.H. Polk, and W.J. Fader, Phys. Fluids 13, 2842 (1970).
8. A.F. Haught, D.H. Polk, J.T. Woo, W.J. Fader, R.G. Tomlinson, R.A. Jong, and W.B. Ard, High-β Capture and Mirror Confinement of Laser-Produced Plasmas, Semi-annual Report, Feb. 1-July 31, 1973 (United Aircraft Corp. UARL-M-921515-19).
9. J. Nuckolls, L. Wood, A. Thiessen, and G. Zimmerman, Nature 239 139 (1972).

10. Thomas R. Jarboe, Study of an Isolated, Laser-Produced Deuterium Plasma in a Magnetic Field, Ph.D. thesis, Lawrence Berkeley Laboratory Report LBL-3097, July 1974.

11. T.R. Jarboe and W. R. Baker, Rev. Sci. Instr. 45, 431 (1974).

12. J.M. Dawson, Phys. Fluids 7, 981 (1964).

13. A.F. Haught and D.H. Polk, Phys. Fluids 9, 2047 (1966).

14. W.J. Fader, Phys. Fluids 11, 2200 (1968).

15. A.F. Haught and D.H. Polk, Phys. Fluids 13, 2825 (1970).

16. M.J. Lubin, H.S. Dunn, and W. Friedman, Heating and Confinement Studies of Laser-Irradiated Solid Particle Plasmas, in Plasma Physics and Controlled Nuclear Fusion Research (International Atomic Energy Agency, Vienna, 1969), Vol. 1, p. 945.

17. M. Mattioli and D. Veron, Phys. Fluids 14, 717 (1971).

18. A. Caruso and R. Gratton, Plasma Phys. 10, 867 (1968).

19. P. Mulser, R. Sigel and S. Witkowski, Physics Reports (Section C of Phys. Letters) 6, 187 (1973).

20. R. Courant and K.O. Friedrichs, Supersonic Flow and Shock Waves (Interscience, New York, 1948).

21. J.L. Bobin, F. Delobeau, G. de Giovanni, C. Fauquignon, and F. Floux, Nucl. Fusion 9, 115 (1969). See also C. Fauquignon and F. Floux, Phys. Fluids 13, 386 (1970).

22. H. Puell, Z. Naturforsch. 25a, 1807 (1970).

23. By asumptotic we mean $t_0 \gg t_b$. t_0 is the time of observing the density distribution. The shape is then independent of t_0, and the expansion is self-similar. See Ya. B. Zel'Dovigh and Yu. P. Raizer, Physics of Shock Waves and High-Temperature Hydrodynamic Phenomena (Academic Press, New York, 1966).

FIGURE LEGENDS

Fig. 1. The pellet is irradiated from the right and ablates on the sides as well as on the back surface (facing the laser).

Fig. 2. Predicted location and density distribution of compressed pellet at various times. The laser beam is incident from the right. After the rarefaction wave reaches the deflagration front, the "pellet" is recompressed. These density plots are found by a simple computer calculation. Note the dramatic shifts in the origins of the position scale. $x = 0$ is the position of the back edge of the pellet at $\tau_b \equiv t/t_b = 0$.

Fig. 3. The velocity of the deflagration front in the hard pellet model compared to the more detailed calculation. Both are one-dimensional calculations.

Fig. 4. Fit of simple theory (——) to the coaxial charge collection data (---) in six directions.

Fig. 5. Asymptotic density distribution for the nonthermally conducting hard-pellet model with $N(\theta_p) \propto \cos^2\theta_p$ and $V(\theta_p) = V_{ex}(1 - 1/3 \sin\theta_p)$. Forward moving cloud produced during late phase is not included.

Fig. 6. The exhaust velocity of the laser-produced plasma as a function of laser power. The solid line is what is expected from the simple model, assuming complete absorption. The large error bars on Φ are caused by uncertainty in laser output and focal spot intensity distribution.

Fig. 7. Burn time measurement of 50-μm deuterium pellets.

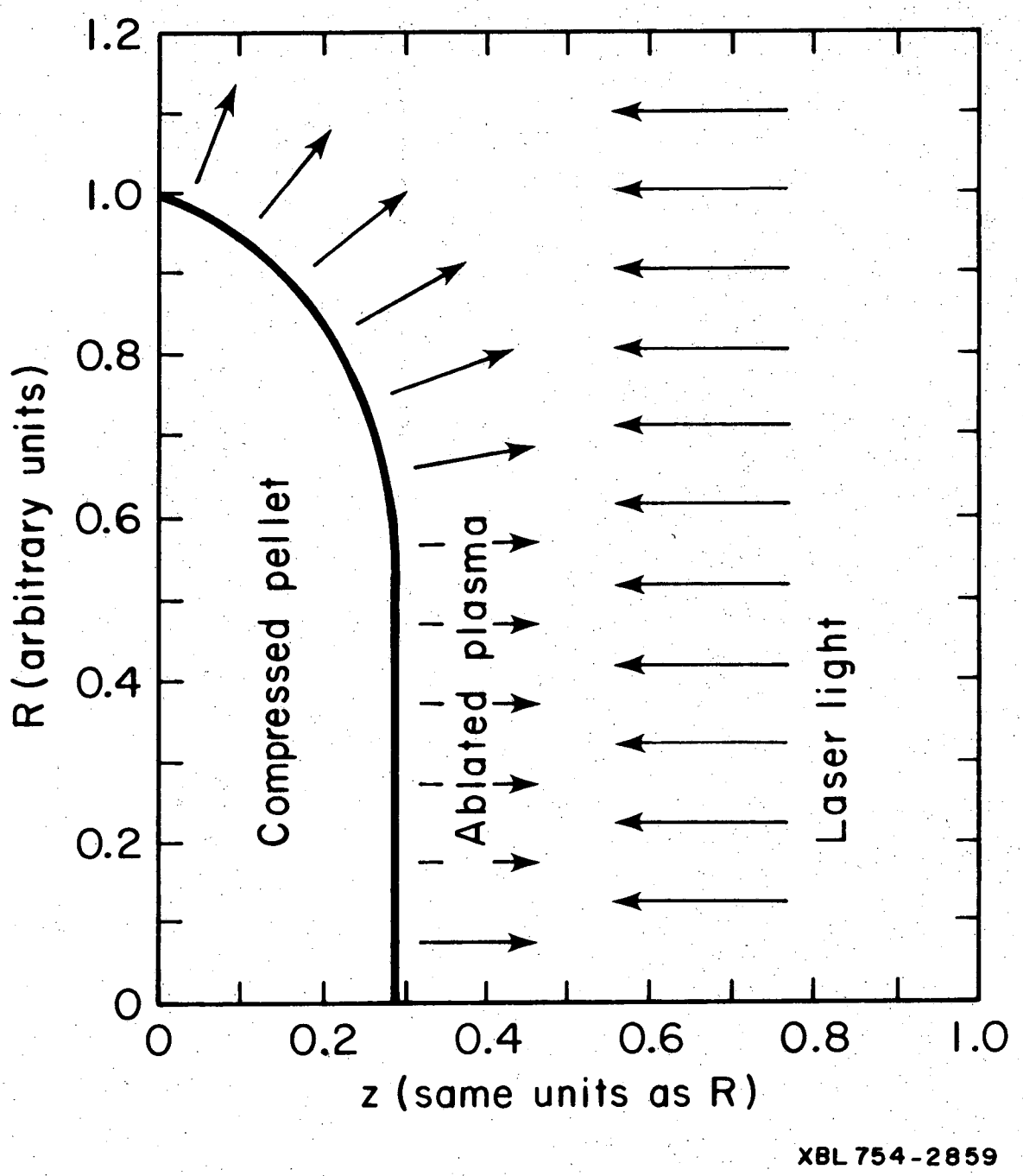
1.2
1.0
0.8
0.6
0.4
0.2
0
R (arbitrary units)
Compressed pellet
Ablated plasma
Laser light
0
0.2
0.4
0.6
0.8
1.0
z (same units as R)
XBL 754-2859

Fig. 1

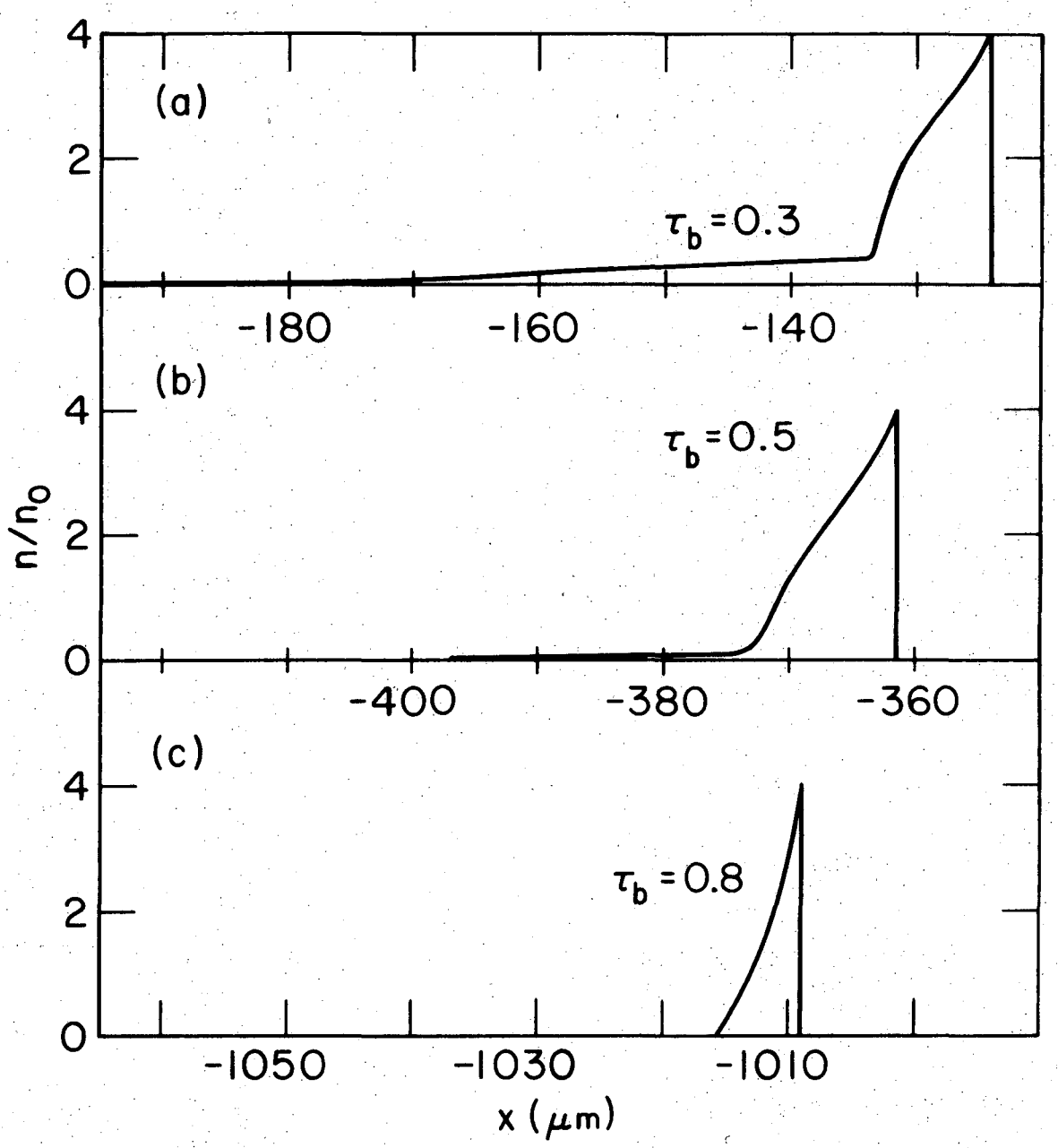

XBL 749-4199 A

Fig. 2

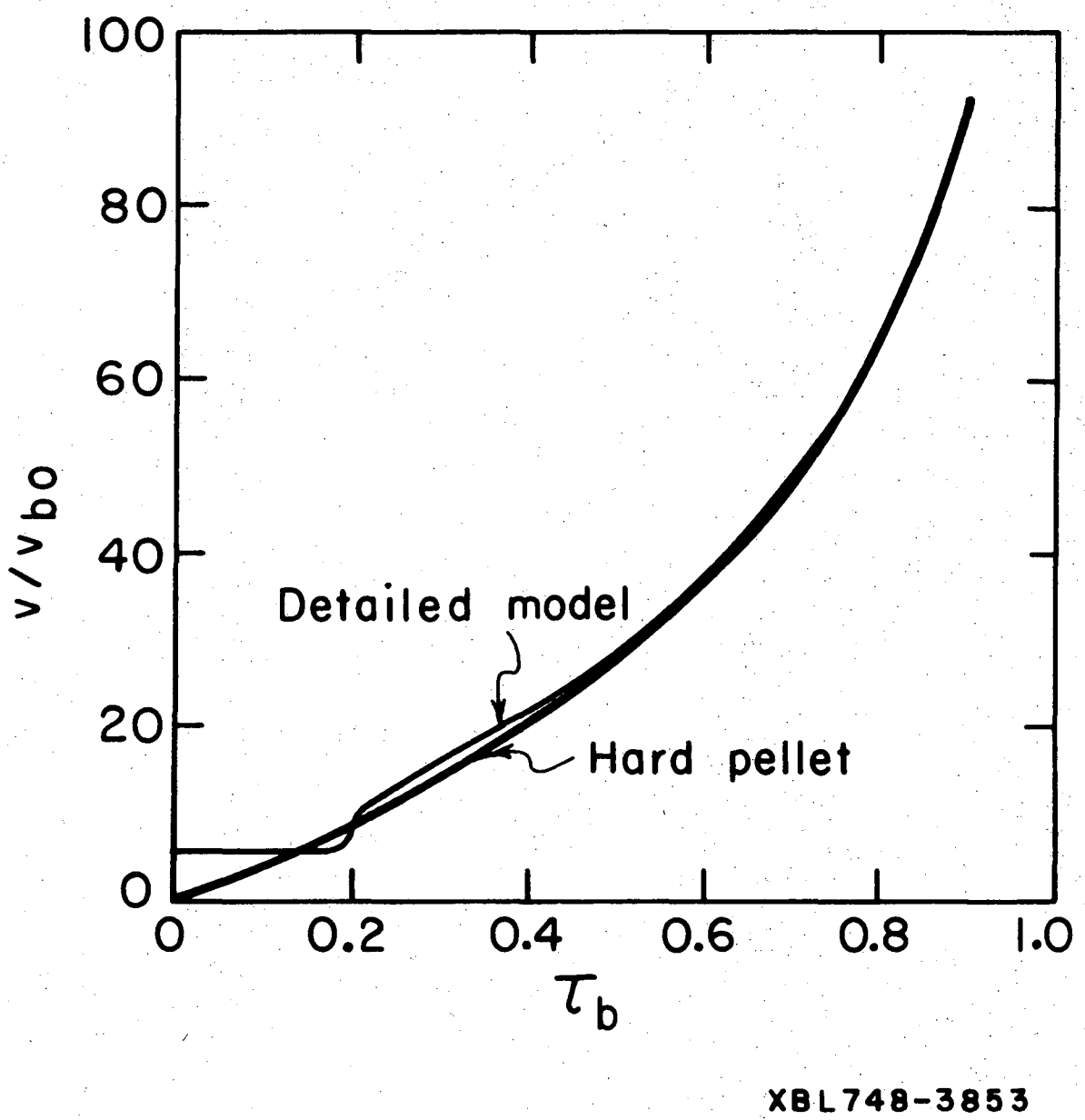
100
80
60
40
20
0
v/v_bo
Detailed model
Hard pellet
0
0.2
0.4
0.6
0.8
1.0
τ_b
XBL748-3853

Fig. 3

0 0 0 0 4 2 0 2 8 3 7

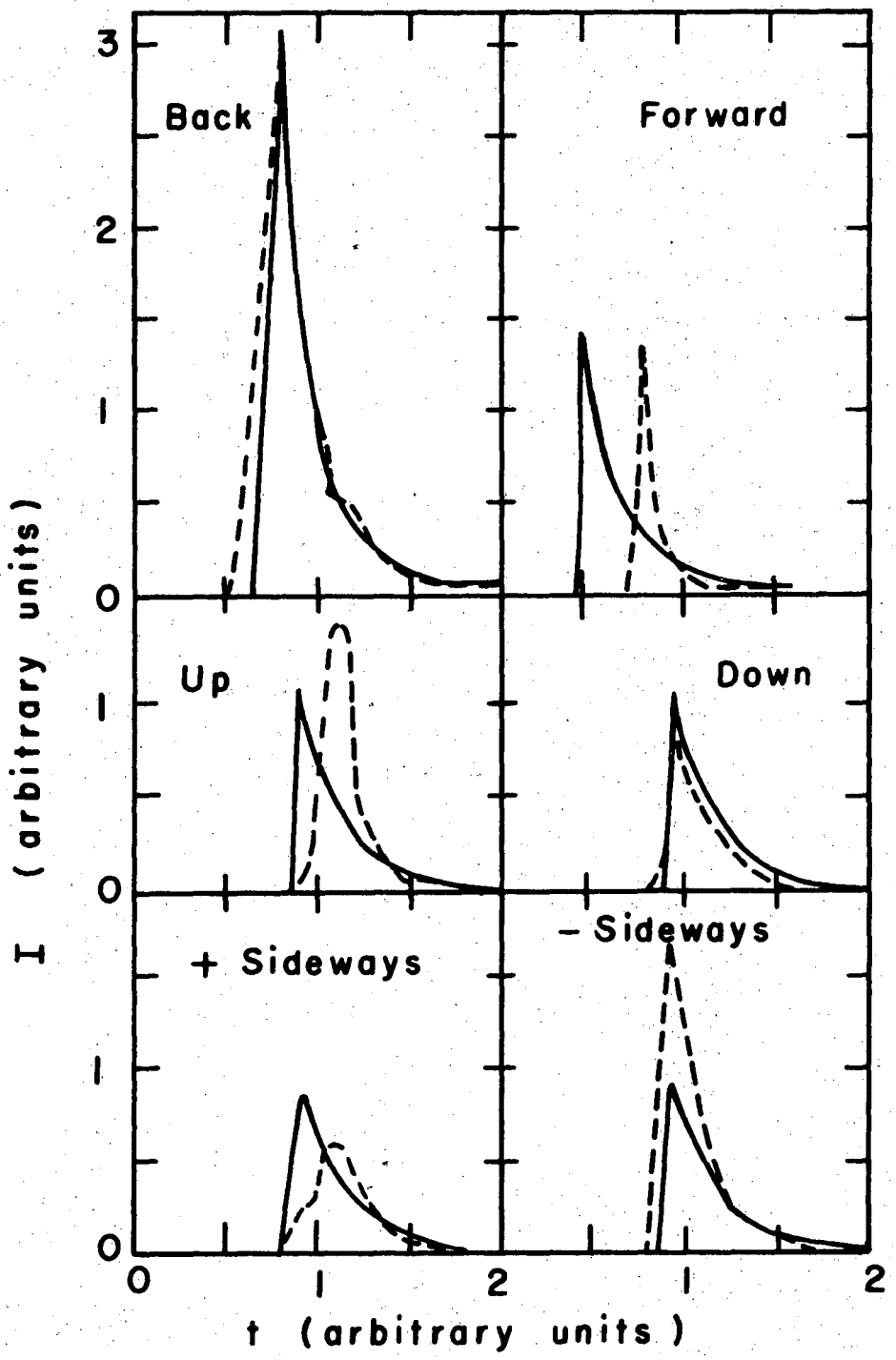

XBL 748-3847

Fig. 4

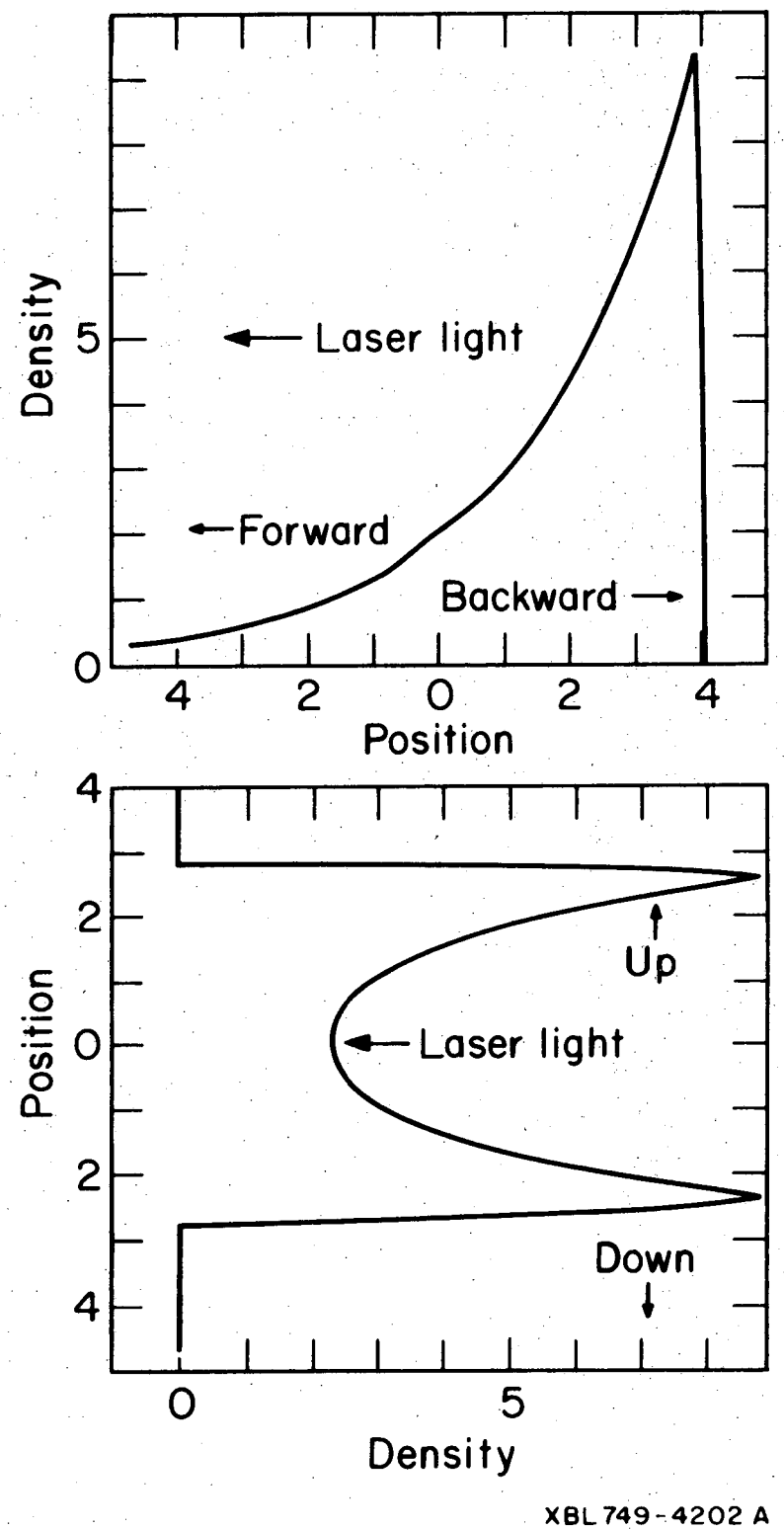
Density
5
0
Laser light
Forward
Backward
4
2
0
2
4
Position
4
2
0
2
4
Position
Up
Laser light
Down
0
5
Density
XBL 749-4202 A

Fig. 5

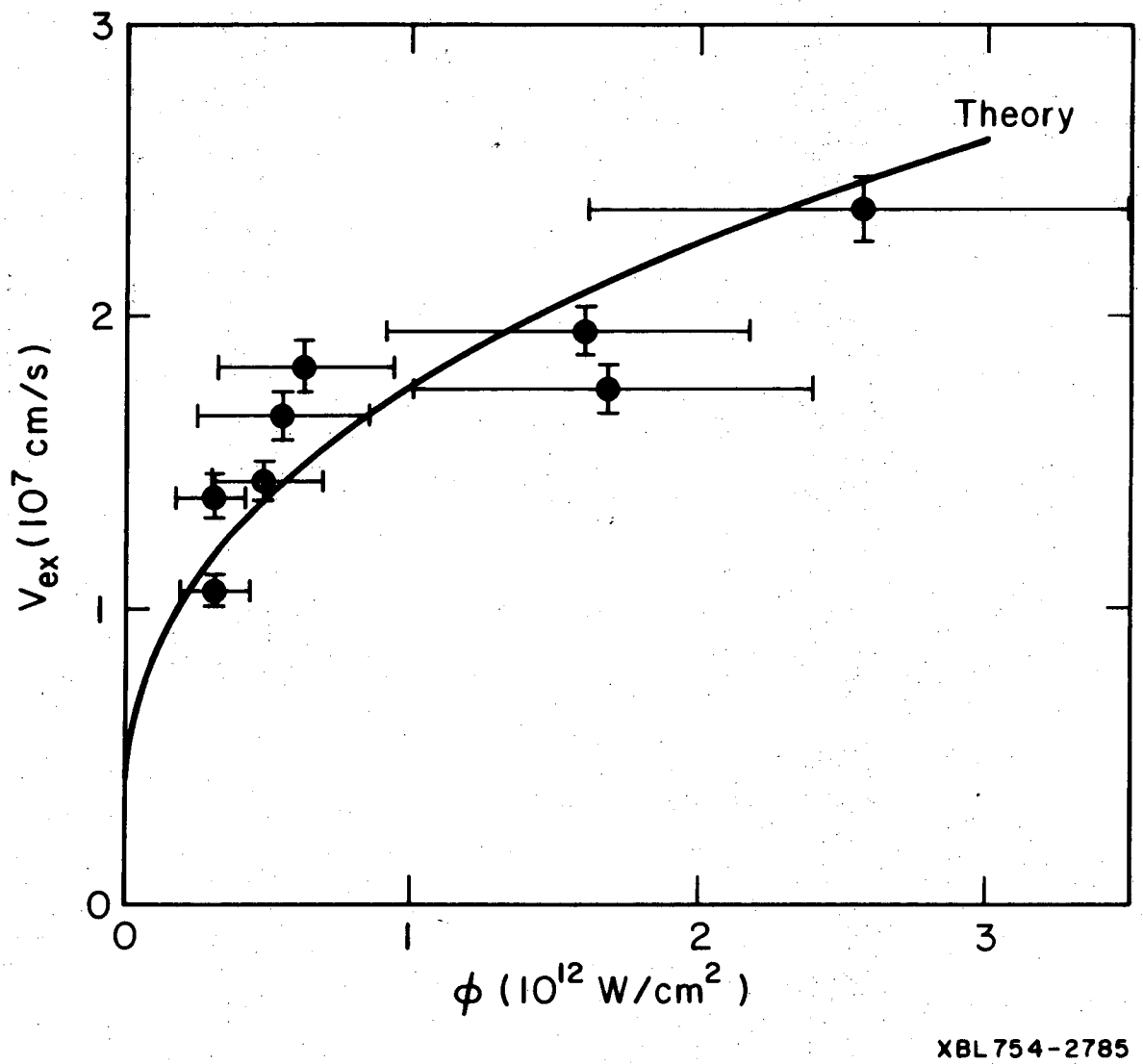

Fig. 6

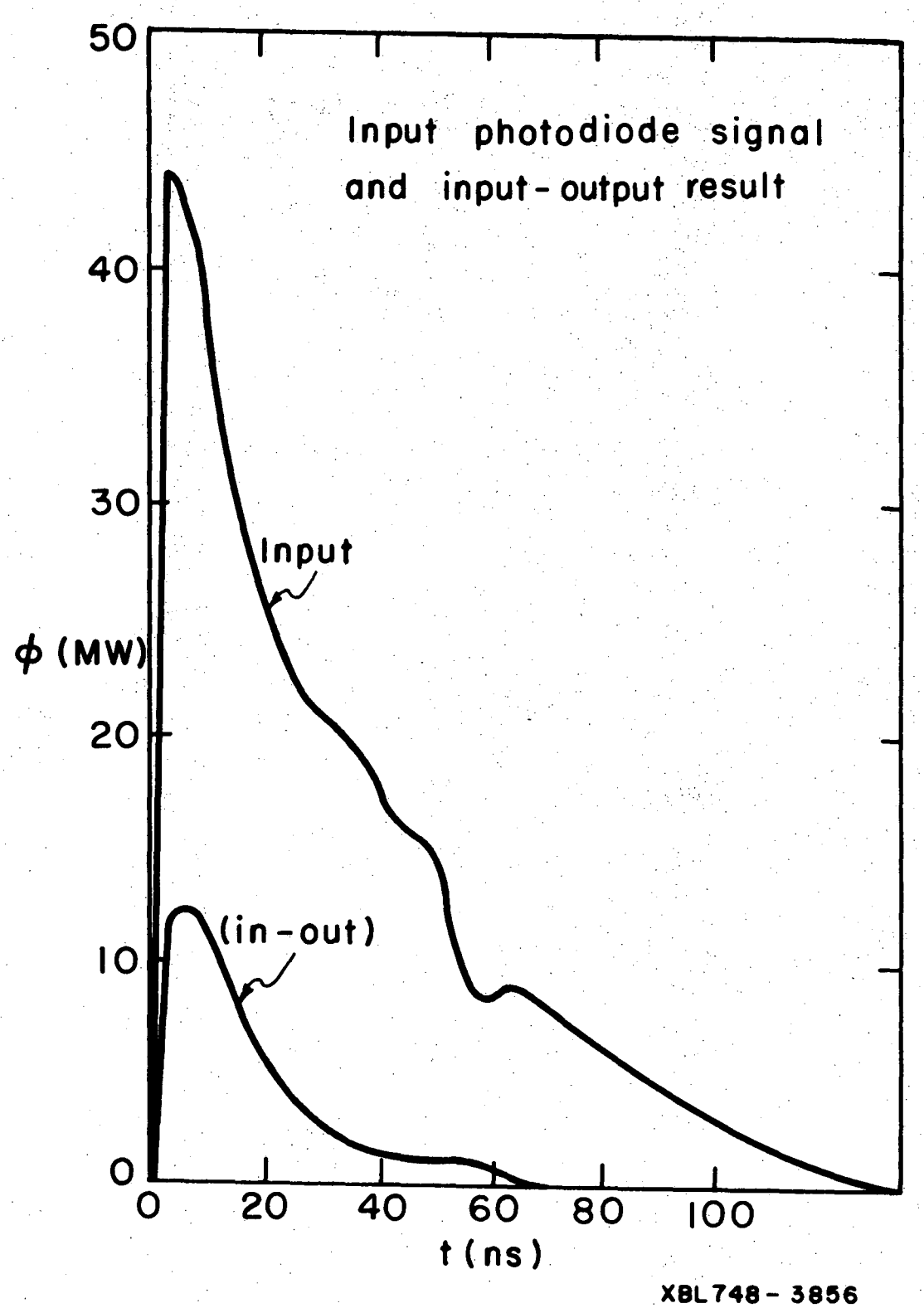
Input photodiode signal
and input-output result
Input
(in-out)
φ (MW)
50
40
30
20
10
0
0
20
40
60
80
100
t (ns)
XBL748-3856

Fig. 7

0 0 0 0 4 2 0 2 8 3 9

LEGAL NOTICE

This report was prepared as an account of work sponsored by the United States Government. Neither the United States nor the United States Energy Research and Development Administration, nor any of their employees, nor any of their contractors, subcontractors, or their employees, makes any warranty, express or implied, or assumes any legal liability or responsibility for the accuracy, completeness or usefulness of any information, apparatus, product or process disclosed, or represents that its use would not infringe privately owned rights.

TECHNICAL INFORMATION DIVISION
LAWRENCE BERKELEY LABORATORY
UNIVERSITY OF CALIFORNIA
BERKELEY, CALIFORNIA 94720